

This document is confidential and is proprietary to the American Chemical Society and its authors. Do not copy or disclose without written permission. If you have received this item in error, notify the sender and delete all copies.

## Spectroscopic Signatures of Resonance Inhibition Reveal Differences in Donor-Bridge and Bridge-Acceptor Couplings

Journal:	<i>Journal of the American Chemical Society</i>
Manuscript ID	ja-2020-00326s.R1
Manuscript Type:	Article
Date Submitted by the Author:	n/a
Complete List of Authors:	Shultz, David; North Carolina State University, Department of Chemistry Kirk, Martin; University of New Mexico, Chemistry Zhang, Jinyuan; Northwestern University Department of Chemistry, Chemistry Stasiw, Daniel; University of Minnesota System, Chemistry Wang, Guangbin; North Carolina State University, Department of Chemistry Yang, Jing; The University of New Mexico, Chemistry and Chemical Biology Habel-Rodriguez, Diana; University of New Mexico, Chemistry Stein, Benjamin; University of New Mexico, Chemistry and Chemical Biology Sommer, Roger; North Carolina State University, Department of Chemistry

SCHOLARONE™  
Manuscripts

# Spectroscopic Signatures of Resonance Inhibition Reveal Differences in Donor-Bridge and Bridge-Acceptor Couplings

David A. Shultz,<sup>1\*</sup> Martin L. Kirk,<sup>2\*</sup> Jinyuan Zhang,<sup>1,a</sup> Daniel E. Stasiw,<sup>1,b</sup> Guangbin Wang,<sup>1,c</sup> Jing Yang,<sup>2</sup> Diana Habel-Rodriguez,<sup>2</sup> Benjamin W. Stein,<sup>2,d</sup> and Roger D. Sommer<sup>1</sup>

<sup>1</sup>Department of Chemistry, North Carolina State University, Raleigh, North Carolina 27695-8204.

<sup>2</sup>Department of Chemistry, The University of New Mexico, MSC03 2060, 1 University of New Mexico, Albuquerque, New Mexico 87131-0001.

Email: shultz@ncsu.edu; [mkirk@unm.edu](mailto:mkirk@unm.edu)

<sup>a</sup>Current address: Beijing National Laboratory for Molecular Sciences, CAS Key Laboratory of Organic Solids, Institute of Chemistry, Chinese Academy of Sciences, Beijing 100190, China

<sup>b</sup>Current address: Cree, Inc., Research Triangle Park, NC

<sup>c</sup>Current address: CombiBlocks, San Diego, CA

<sup>d</sup>Current address: Los Alamos National Laboratory, Los Alamos, NM

**KEYWORDS.** Donor-acceptor, exchange coupling, electronic coupling, biradical, dioxolene, steric inhibition of resonance, configuration interaction

## Supporting Information Placeholder

**Abstract:** The torsional dependence of the ground state magnetic exchange coupling ( $J$ ), and the corresponding electronic coupling matrix element ( $H_{DA}$ ) for eight transition metal complexes possessing donor-acceptor (D-A) biradical ligands is presented. These biradical ligands are comprised of an  $S = \frac{1}{2}$  metal semiquinone (**SQ**) donor and an  $S = \frac{1}{2}$  nitronyl nitroxide (**NN**) acceptor, which are coupled to each other via *para*-phenylene, methyl-substituted *para*-phenylenes, or bicyclo[2.2.2]octane ring. The observed trends in electronic absorption and resonance Raman spectral features are in accord with reduction in electronic and magnetic coupling between D and A units within the framework of our valence bond configuration interaction model. Moreover, our spectroscopic results highlight different orbital mechanisms that modulate coupling in these complexes, that is not manifest in the ferromagnetic  $J_{SQ-B-NN}$  values. The work provides new detailed insight into the effects of torsional rotations which contribute to inhomogeneities in experimentally determined exchange couplings, electron transfer rates, and electron transport conductance measurements.

## Introduction

Persistent Donor-Bridge-Acceptor (D-B-A) biradicals offer a unique and instructive platform to elucidate mechanisms of bridge-mediated electronic coupling, which is central to our understanding of orbital pathways that contribute to molecular superexchange-mediated electron transfer and electron transport in single-molecule electronic devices. The importance of electronic coupling has been recently highlighted as a transferable property of the bridge moiety that directly relates superexchange (*i.e.*

magnetic exchange coupling) to photoinduced electron transfer rates, and electron transport (conductance) mediated by molecular bridges.<sup>1</sup> Prior work from our laboratories has made extensive use of X-ray crystallography, magnetic susceptibility measurements, optical and magnetic spectroscopies, and electronic structure computations to elucidate electronic and geometric structure contributions to magnetic exchange coupling and electronic coupling in D-B-A systems where the donor (D) is a semiquinone radical (D = SQ; S = ½), the acceptor (A) is the nitronyl nitroxide radical (A = NN; S = ½), and the bridge (B) can be any synthetically-viable molecular fragment.<sup>2-8</sup> The presence of a single, dominant  $\pi$ -superexchange pathway connecting SQ and NN allows one to evaluate the relationship between magnetic exchange coupling,  $J_{SQ-B-NN}$ , and electronic coupling ( $H_{SQ-B-NN}$ ) using experimental observables in the context of a valence bond configuration interaction (VBCI) model, Eqn. 1 and Fig. 1. For the systems described here,  $J_{DA} \equiv J_{SQ-B-NN}$  and  $H_{DA} \equiv H_{SQ-B-NN}$  and the spectroscopic observables<sup>7</sup> are the mean SQ  $\rightarrow$  B-NN charge transfer (CT) energy ( $U$ ) and the CT excited state singlet-triplet gap ( $K_0$ ).

$$J_{DA} = \frac{H_{DA}^2 K_0}{U^2 - K_0^2} \quad (1)$$

An intense SQ( $\pi$ )  $\rightarrow$  B-NN( $\pi^*$ ) intraligand charge transfer (ILCT) transition is a defining spectroscopic feature that is characteristic of an established contiguous  $\pi$ -communication pathway in these D-B-A biradicals. Configurational mixing of the ILCT excited state into the electronic ground state contributes to the magnitude of  $J_{SQ-B-NN}$  (i.e. the ground singlet-triplet gap,  $\Delta_{S-T} = 2J_{SQ-B-NN}$ ),<sup>4, 5, 7</sup> which is a fit parameter in the analysis of D-A biradical variable-temperature magnetic susceptibility data. Since  $J_{SQ-B-NN}$  is proportional to  $H_{DA}^2$ , for a given SQ-Bridge-NN complex the electronic coupling can be determined conveniently from the ratio  $J_{SQ-B-NN}/J_{SQ-NN}$  ( $=H_{SQ-B-NN}^2/H_{SQ-NN}^2$ ).<sup>4, 5, 7</sup> Here,  $J_{SQ-NN}$  is the magnitude of the non-bridged "parent" biradical complex for which both  $J_{SQ-NN}$  and  $H_{SQ-NN}$  have been determined from detailed magnetic and spectroscopic studies.<sup>2, 5, 7</sup> Moreover, due to the persistent nature of these biradicals,  $H_{SQ-B-NN}$  and  $J_{SQ-B-NN}$  can be directly correlated with crystallographically-determined bond lengths, bond torsion angles, and the distance between the donor and acceptor fragments. We have shown that  $J_{SQ-B-NN}$  decays exponentially as a function of distance ( $r_{SQ-NN}$ ) for oligo-thiophene and oligo-phenylene bridges, and the experimentally determined decay constants ( $\beta$ ) are in agreement with those determined from electron transfer kinetics, in accord with a bridge mediated superexchange pathway.<sup>2</sup>

The degree of  $\pi$ - $\pi$ -orbital overlap in conjugated D-B-A systems plays a defining role in modulating the resultant electronic coupling. Wasielewski has shown<sup>9</sup> using oligo(phenylene-ethylene)-bridged donor-acceptor molecules that the magnitude of  $H_{DA}$  is related to the torsion angles between the D, B, and A fragments, and the electronic coupling possesses a  $\cos(\phi)$  dependence for each fragment-fragment bond torsion within a D-B-A photoinduced electron transfer (PET) system. Similarly, work by Mayor<sup>10</sup> has shown a bond torsion dependence on the magnitude of the conductance ( $g$ ) in molecular systems. Additionally, Harriman<sup>11</sup> and Wenger<sup>12</sup> have shown that PET rates vary as a function of the torsional dependence of  $H_{DA}$ , while Newton described an extended McConnell relationship<sup>13</sup> that accounts for both  $\sigma$  - and  $\pi$ -contributions to electronic coupling.<sup>14</sup> Using SQ-Bridge-NN donor-acceptor biradical complexes, we have recently shown that the magnitude of the electronic and magnetic exchange couplings as a function of bridge torsion angles span a well-described, smooth 3D surface.<sup>15</sup> These results are important since they show that the  $\pi$ -contribution to electronic coupling is  $\sim 13$  times greater than the  $\sigma$ -coupling pathway, in accord with theory.<sup>16, 17</sup> In this manuscript, we detail how electronic absorption and resonance Raman

spectroscopies can be used in conjunction with magnetic susceptibility measurements to develop a more comprehensive understanding of steric inhibition of resonance<sup>18, 19</sup> in torsionally-rotated Donor-Bridge-Acceptor biradicals.

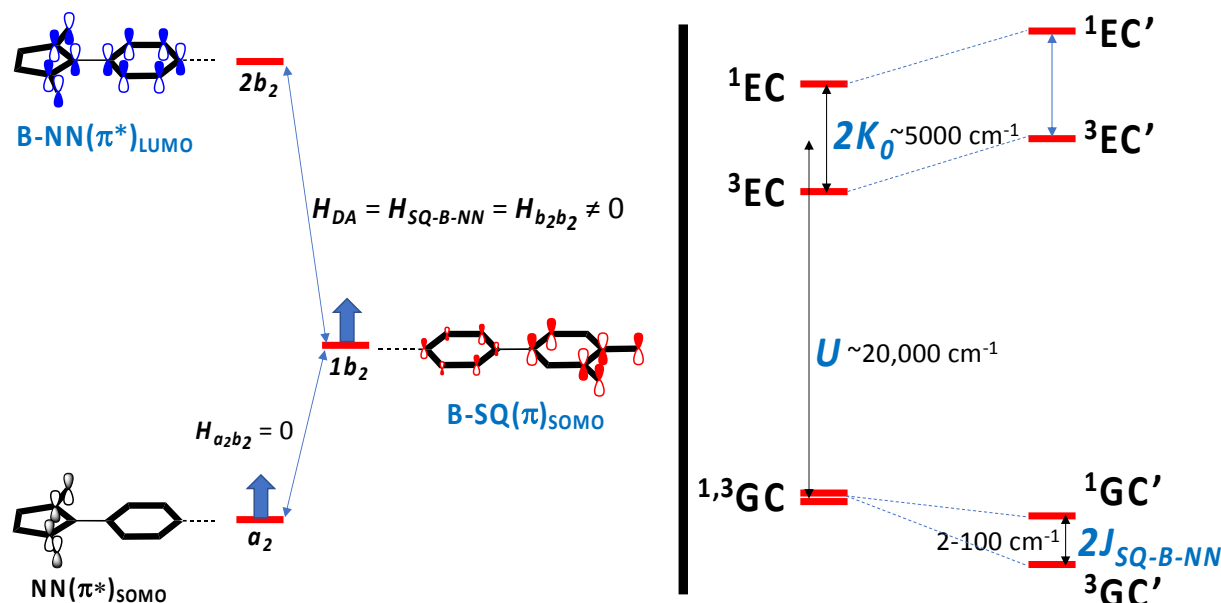


**Figure 1.** Left: Frontier NN(SOMO), SQ(SOMO) and NN(LUMO) orbitals fragments utilized in the VBCI model, right. Note that both the SQ(SOMO) and the NN(LUMO) have bridge character, provided that the corresponding torsion angles are less than  $90^\circ$ . Right: VBCI model illustrating SQ  $\rightarrow$  B-NN CT configurations ( $^1EC$  and  $^3EC$ ;  $a_2^1b_2^02b_2^1$ ) that mix with corresponding ground configurations ( $^1GC$  and  $^3GC$ ;  $a_2^1b_2^12b_2^0$ ) to create the experimentally-evaluated singlet-triplet gap ( $2J_{SQ-B-NN}$ ).

## Result and Discussion

**Molecular Structures and Conformations.** Our previous report on the torsional dependence of electronic and exchange coupling lacked critical data points corresponding to structures with large donor torsion and small acceptor torsion relative to the bridge, and *vice versa*. Thus, to complete this series of complexes, we prepared **1-Me<sub>2</sub>Ph** and **1-PhMe<sub>2</sub>** (see SI for synthetic and crystallographic details) using our standard procedures.<sup>2, 3, 15, 20</sup> These two new complexes possess the desired conformations, Fig.2, for selectively and independently reducing D-B and B-A electronic couplings. For comparison, also shown in Fig. 2, are the bond-line drawings and thermal ellipsoid plots of **1-Ph**, **1-MePh**, **1-PhMe**, **1-*p*-MePhMe**, **1-Me<sub>2</sub>PhMe<sub>2</sub>** and **1-BCO** that have been previously reported. Torsion angles for the (substituted) phenylene-bridged biradical complexes were determined using the mean planes of the SQ rings and bridge rings ( $\phi_{SQ}$ ), and the O-N-C-N-O plane of NN and mean plane of the bridge rings ( $\phi_{NN}$ ). These data are provided in Fig. 2.

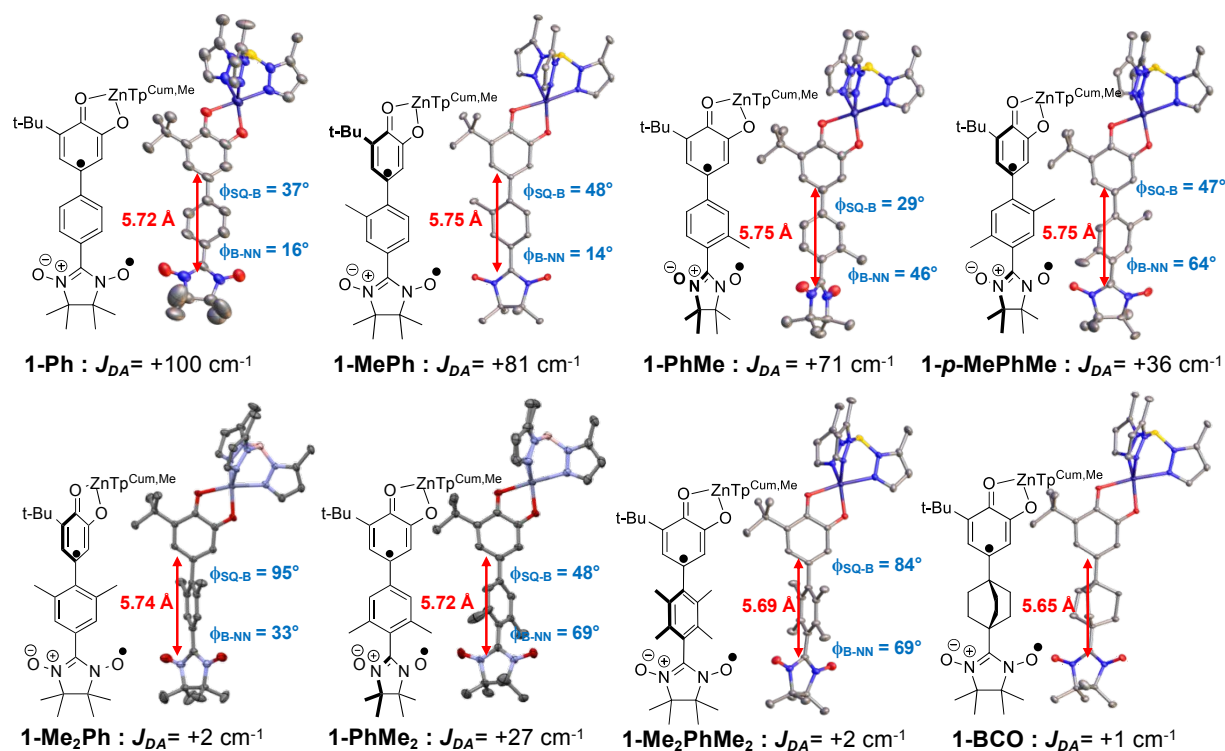


**Figure 2.** Bond-line drawings, thermal ellipsoid plots (cumenyl groups of the ancillary ligand, hydro-tris(3,5-dimethylpyrazolyl)borate (Tp<sup>Cum,Me</sup>)<sup>21, 22</sup> and hydrogen atoms have been omitted for clarity), donor-bridge and acceptor-bridge torsion angles (rounded off to the nearest degree), donor-acceptor distances and  $J_{SQ-B-NN}$  exchange parameters (rounded off to the nearest wavenumber) of complexes studied in this work. Complexes **1-Me<sub>2</sub>Ph** and **1-PhMe<sub>2</sub>** were prepared for this study.

**Effects of Steric Inhibition of Resonance Conjugation on Magnetic Exchange Coupling.** Since both the SQ and NN radicals are  $S=1/2$  spin-bearing units, the relative magnitudes of the bridge-mediated SQ-NN electronic coupling ( $H_{SQ-B-NN}$ ) in our series of complexes can be determined conveniently at high resolution by measuring the relative magnitudes of their respective bridge-mediated SQ-NN magnetic exchange interactions,  $J_{SQ-B-NN}$ .<sup>5, 7, 23-26</sup> This can be accomplished using temperature- or magnetic field-dependent spectroscopies (e.g., electronic absorption spectroscopy<sup>5,27</sup> or EPR,<sup>28</sup>) or magnetic susceptibility measurements with the singlet-triplet exchange splitting being equal to  $2J_{SQ-B-NN}$  according to the Heisenberg exchange Hamiltonian, Eqn. (2):

$$\mathcal{H}_{SQ-B-NN} = -2J_{SQ-B-NN}\hat{S}_1\cdot\hat{S}_2 \quad (2)$$

where the individual  $\hat{S}_i$  are the spin operators for the  $S=1/2$  radical spins. Magnetic susceptibility data, plotted as the  $\chi_{para}\cdot T$  product vs. temperature for the two new complexes (**1-Me<sub>2</sub>Ph** and **1-PhMe<sub>2</sub>**) are displayed in Fig. 3 (see SI for additional magnetic data). Best fits (derived from Eq. (2), see SI) to the data yield  $J_{1-PhMe_2} = +27 \pm 2\text{ cm}^{-1}$  and  $J_{1-Me_2Ph} = +1.5 \pm 0.1\text{ cm}^{-1}$ .

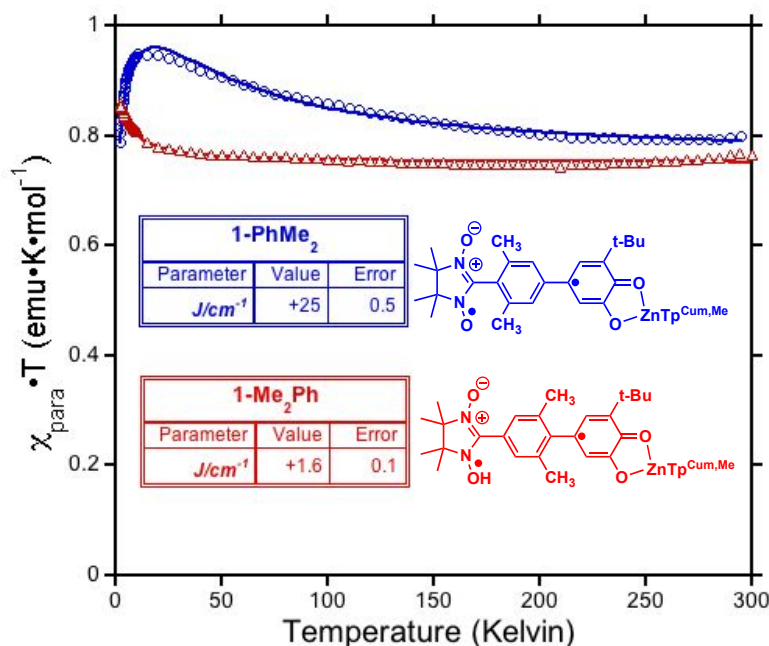


**Figure 3.** Variable-temperature magnetic susceptibility plots displayed as  $\chi_{\text{para}} \cdot T$  vs.  $T$  plots for the two new complexes, **1-PhMe<sub>2</sub>** (○) and **1-Me<sub>2</sub>Ph** (Δ). Fits include a weak, antiferromagnetic intermolecular Weiss correction of -0.51 K (**1-PhMe<sub>2</sub>**), and -0.28 K (**1-Me<sub>2</sub>Ph**), see SI.

The McConnell superexchange model defines  $H_{DA}$  as the product of the electronic coupling matrix elements that describes the pairwise interactions ( $H_{DB}$ ,  $H_{BA}$ ) within a D-B-A triad divided by the energy gap between the localized donor and bridge states ( $\Delta_{DB}$ ) as shown in Eqn. 3.<sup>13</sup>

$$H_{DA} = \frac{H_{DB}H_{BA}}{\Delta_{DB}} \quad (3)$$

When the dominant electronic coupling occurs through a series of  $\pi$ -systems connected by  $\sigma$ -bonds, there is a torsional dependence of  $H_{DB}$  and  $H_{BA}$  that is described by Eqn. 4, where  $i$  and  $j$  index two adjacent  $\pi$ -units of the D-B-A system and  $H_{ij}^0$  is the intrinsic electronic coupling matrix element at  $\cos\phi = 0$ , where the constituent  $\pi$ -systems are coplanar.<sup>9,11</sup>

$$H_{ij} = H_{ij}^0 \cos\phi \quad (4)$$

Since  $J_{SQ-B-NN}$  varies as  $H_{SQ-B-NN}^2$  (Eqn. 1) there will be a  $\cos^2\phi$  dependence for  $J_{SQ-B-NN}$ . It is clear from the data in Table 1 that the  $H_{SQ-B-NN}$  coupling requires a strong interaction of the bridge with *both* SQ/donor and NN/acceptor orbitals. Consider the data in Table 1 for complexes **1-MePh** and **1-*p*-MePhMe**. These two complexes have nearly equal SQ-B bond torsions (48° and 47°, respectively), but quite different B-NN bond torsions (14° and 64°, respectively). As a result,  $H(\mathbf{1-MePh}) \sim 1.5H(\mathbf{1-p-MePhMe})$ . We now compare the data for complexes **1-PhMe<sub>2</sub>** and **1-Me<sub>2</sub>PhMe<sub>2</sub>**. These two complexes have nearly equal B-NN bond torsions (70° and 69°, respectively), but quite different SQ-B bond torsions (48° and 84°, respectively). As

a result,  $H(1\text{-PhMe}_2) \sim 13H(1\text{-Me}_2\text{PhMe}_2)$ . These results are conveniently illustrated graphically, and a plot of magnetic exchange,  $J_{\text{SQ-B-NN}}$  versus the product of the cosine-squared of the SQ-Ph and Ph-NN torsion angles ( $\phi_{\text{SQ-B}}$  and  $\phi_{\text{B-NN}}$ , respectively, Fig. 2 and Table 1) are provided in Fig. 4.<sup>15</sup> The two new complexes occupy weaker coupling regions of the surface map.

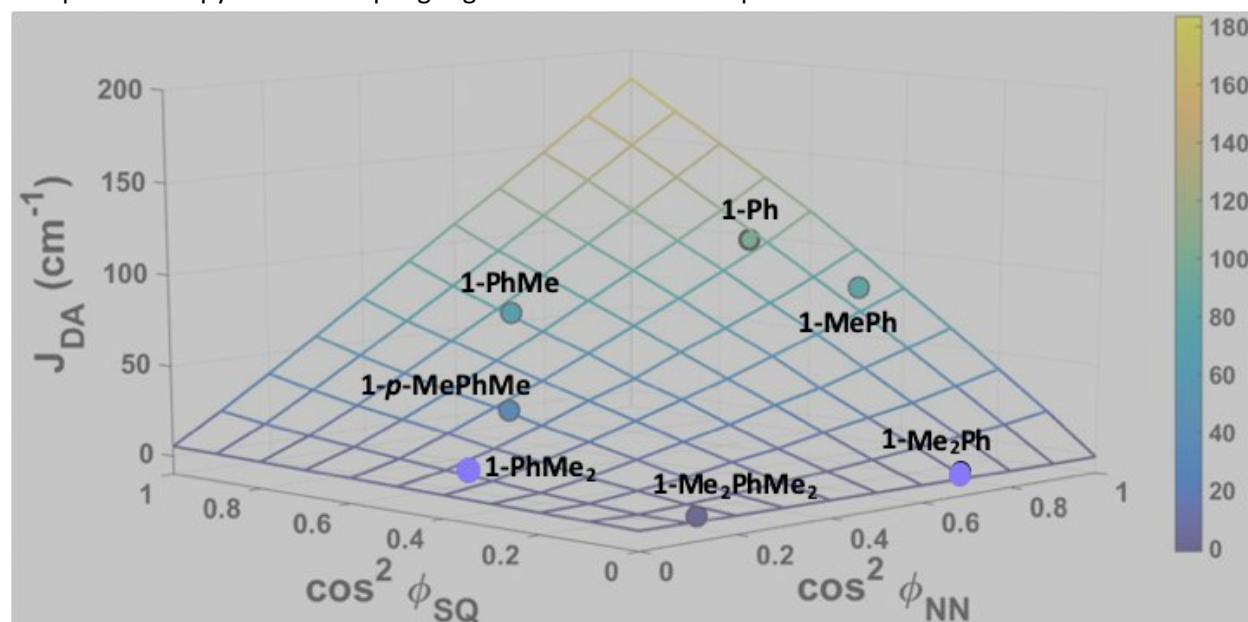


**Figure 4.** Experimental change coupling values vs. the cosine-squared of torsion angles for SQ-Ph and Ph-NN. Square-blocked grid correlates experimental  $J_{\text{SQ-B-NN}}$  values with experimental SQ-Ph and Ph-NN torsion angles:  $J_{\text{SQ-B-NN}} = 0.34 + 3.77 \cdot \cos^2(\phi_{\text{SQ-Ph}}) - 13.4 \cdot \cos^2(\phi_{\text{Ph-NN}}) + 179 \cdot \cos^2(\phi_{\text{SQ-Ph}}) \cdot \cos^2(\phi_{\text{Ph-NN}}) + 16.3 \cdot \cos^4(\phi_{\text{Ph-NN}})$ . See SI for error analysis.

*Steric Inhibition of Resonance Conjugation Probed by Electronic Absorption and Resonance Raman Spectroscopies.* The auxochromic methyl groups, although sterically rather small ( $d \sim 2\text{\AA}$ ),<sup>29</sup> are effective at rotating independently or collectively the **SQ** donor relative to the bridge (**1-MePh**, **1-p-MePhMe**, **1-Me₂Ph** and **1-Me₂PhMe₂**) as well as the **NN** acceptor relative to the bridge (**1-PhMe**, **1-p-MePhMe**, **1-PhMe₂** and **1-Me₂PhMe₂**), Fig.2 and Table 1. When either the SQ or NN moieties are “flanked” by two methyl groups they are rotated so that their  $\pi$ -systems are nearly orthogonal to those of the phenylene bridge (**1-Me₂Ph**, **1-PhMe₂** and **1-Me₂PhMe₂**) (Table 1). Due to steric differences between the two radicals, two *ortho*-methyl groups are less effective at rotating the NN than they are at rotating the SQ. The smaller internal bond angles of the 5-membered NN ring compared to those of a 6-membered ring contributes to this effect. The attenuation of conjugation across the D-B-A triad that results from steric interactions between methyl groups and the SQ and NN radicals dramatically attenuates the magnetic exchange coupling in this series of biradicals, and this inhibition of resonance is also manifest in the different electronic absorption spectra of these complexes (Fig. 5). While all the spectra are characterized by absorption bands originating from the constituent chromophores (SQ,  $\sim 12000\text{ cm}^{-1}$ ; 840 nm and NN,  $\sim 17200\text{ cm}^{-1}$ ; 580 nm,  $\sim 27000\text{ cm}^{-1}$ ; 370 nm),<sup>30, 31</sup> only those complexes with effective donor-bridge-acceptor extended  $\pi$ -conjugation exhibit a charge transfer transition of varying intensity at  $\sim 23000\text{ cm}^{-1}$  ( $\sim 435\text{ nm}$ ).



Comparison of these six spectra show that complexes with methyl groups that can interfere sterically with the NN acceptor possess ILCT bands with attenuated intensity that are overlapped with broadened or shifted 27000 cm<sup>-1</sup> B-NN( $\pi \rightarrow \pi^*$ ) bands. The electronic absorption spectra for these eight compounds can be grouped into three categories: A, B, and C. Category A (Table 1, Fig. 5A) is exemplified by **1-Ph**, **1-MePh**, and, **1-Me<sub>2</sub>Ph**, and inspection of their geometric structures indicates that they will display the highest degree of Ph-NN  $\pi$ -conjugation in the series since there is no methyl group steric interference with the NN moiety. Complex **1-Ph** has an unsubstituted *para*-phenylene bridge and exhibits an intense intraligand charge transfer (ILCT) band near 23000 cm<sup>-1</sup>. This band has been probed extensively by a combination of electronic absorption, resonance Raman (rR), and hot band spectroscopies. Additional insight into the nature of this transition has been obtained within the context of DFT and TD-DFT computations leading to the rigorous assignment of this band as possessing appreciable intraligand SQ( $\pi$ )  $\rightarrow$  B-NN( $\pi^*$ ) charge transfer (ILCT) character.<sup>3-5, 7, 15</sup> Thus, the presence of an ILCT band in this energy region is a hallmark of extended donor-bridge-acceptor  $\pi$ -conjugation in SQ-B-NN biradicals. A similar ILCT band is observed for **1-MePh**, but it is slightly blue-shifted and possesses reduced intensity when compared to **1-Ph**. The ILCT band in **1-MePh** retains the vibronic structure observed in **1-Ph**, which is associated with an excited state distortion along in-plane SQ, NN, and phenylene vibrational modes.<sup>5</sup> The ILCT band assignment for **1-Ph** and **1-MePh** is also supported by their respective resonance Raman spectra and excitation profiles, *vide infra*. We observe a precipitous decrease in the ILCT band intensity for **1-Me<sub>2</sub>Ph** since the phenylene bridge is rotated orthogonal to the SQ plane ( $\phi_{SQ-Bridge} = 95^\circ$ ), and this leads to a loss of extended conjugation connecting SQ with NN across the SQ-B-NN structure. At higher energies than the ILCT band, all of the Category A complexes display a distinct, structured CT band at ~27,500 cm<sup>-1</sup> with virtually unchanged intensity across the series. We assign this band as the NN(SOMO)  $\rightarrow$  Ph-NN(LUMO) + Ph-NN(HOMO)  $\rightarrow$  NN(SOMO) transition on the basis of the earlier spectral assignments made for Tp<sup>Cum,Me</sup>Cu(SQ-NN), Tp<sup>Cum,Me</sup>Cu(SQ-*m*-Ph-NN) and Ph-NN,<sup>7</sup> the results of TD-DFT computations,<sup>30</sup> and the fact that **1-Ph**, **1-MePh**, and, **1-Me<sub>2</sub>Ph** all lack steric interference that would result in inhibition of resonance between the phenylene bridge and the NN radical. Remarkably, the electronic absorption spectrum of **1-Me<sub>2</sub>Ph** is strikingly similar to **1-*m*-Ph**, which possesses a cross-conjugated *meta*-phenylene bridge (*m*-Ph).<sup>3</sup> Thus, the loss of Ph-NN conjugation as a function of torsional rotation produces a similar effect to cross-conjugation with respect to the loss of SQ $\rightarrow$ B-NN ILCT intensity.

**Table 1.** Magnetic Exchange ( $J_{SQ-B-NN}$ ) and Electronic Coupling ( $H_{SQ=B-NN}$ ) Constants for Methyl-Substituted, Phenylene-Bridged SQ-NN Biradical Complexes.

Compound	Category	$\phi_{SQ-Bridge} (^\circ)$	$\phi_{Bridge-NN} (^\circ)$	$J_{SQNN} (cm^{-1})$	$H_{SQNN} (cm^{-1})^{a,b}$	Reference
<b>1-Ph</b>	<b>A</b>	37	16	100	3632	5, 20
<b>1-MePh</b>		48	14	81	3269	15
<b>1-Me<sub>2</sub>Ph</b>		95	33	2	514	This Work
<b>1-PhMe</b>	<b>B</b>	29	46	71	3060	15
<b>1-<i>p</i>-MePhMe</b>		47	64	36	2179	15
<b>1-PhMe<sub>2</sub></b>		48	69	27	1816	This Work
<b>1-Me<sub>2</sub>PhMe<sub>2</sub></b>	<b>C</b>	84	69	2	514	15
<b>1-BCO</b>		NA	NA	1	363	15



<sup>a</sup>Electronic couplings determined by ratio with **1-Ph** for which  $H_{SQ-B-NN}$  was determined by VBCI matrix diagonalization.<sup>5</sup> <sup>b</sup>Although the superexchange pathways for **1-Me<sub>2</sub>Ph**, **1-Me<sub>2</sub>PhMe<sub>2</sub>** and **1-BCO** may be/are dominated by  $\sigma$ -bonds, their electronic couplings are computed by ratio with **1-Ph** for comparison.

Category B compounds (Table 1, Fig. 5B) include **1-PhMe**, **1-*p*-MePhMe**, and **1-PhMe<sub>2</sub>**, which display electronic absorption spectra that are all quite similar. The Category B compounds possess a marked decrease in Ph-NN  $\pi$ -conjugation when compared with the Category A compounds due to the increased torsional rotation about the Ph-NN bond. The reduction in Ph-NN  $\pi$ -conjugation leads to charge transfer absorption features being shifted to higher energy with respect to the Category A compounds. TDDFT computations on **1-PhMe<sub>2</sub>** indicate electronic transitions responsible for the absorption band centered at  $\sim 26,000$   $\text{cm}^{-1}$  possess contributions from  $SQ \rightarrow B-NN$  and  $B-NN \rightarrow SQ$  one-electron promotions, both of which serve to promote magnetic exchange coupling between the SQ and NN spins within a VBCI model. The rather dramatic differences in spectral features for **1-MePh** and **1-PhMe** indicate that bridge-acceptor conjugation plays a greater role in ILCT band energy and intensity than does donor-bridge conjugation.<sup>6</sup> Thus, the electronic absorption spectra can distinguish between these two bond torsion effects at near parity of the exchange coupling (e.g. **1-MePh** vs. **1-PhMe**). Here, population of the Ph-NN  $\pi^*$  LUMO via a one-electron promotion creates the ILCT state (Fig. 1). The vibronic structure associated with the  $NN(SOMO) \rightarrow Ph-NN(LUMO) + Ph-NN(HOMO) \rightarrow NN(SOMO)$  transition is observed on the high energy side of the broad CT feature for **1-PhMe** and **1-MePhMe** at  $\sim 27,500$   $\text{cm}^{-1}$ . Intensity in this region is diminished in **1-PhMe<sub>2</sub>** due to increased torsional rotation about the Ph-NN bond leading to a loss of conjugation.

The category C (Table 1, Fig. 5C) compounds are comprised of **1-Me<sub>2</sub>PhMe<sub>2</sub>** and **1-BCO**, for which both SQ and NN radical  $\pi$ -systems are decoupled due to either the complete absence of a  $\pi$ -system bridge (**1-BCO**) or large SQ-Ph and Ph-NN bond torsions that effectively eliminate donor-acceptor  $\pi$ -conjugation in **1-Me<sub>2</sub>PhMe<sub>2</sub>**. Thus, neither **1-Me<sub>2</sub>PhMe<sub>2</sub>** nor **1-BCO** (Fig. 5C) possess strong charge transfer absorbance features in the ILCT region of the spectrum or in the higher energy (*i.e.*  $27,000$   $\text{cm}^{-1}$ )  $NN(SOMO) \rightarrow Ph-NN(LUMO) + Ph-NN(HOMO) \rightarrow NN(SOMO)$  region of the spectrum. This observation is fully consistent with complete electronic and magnetic  $\pi$ -decoupling of the spin-bearing units and dramatically reduced exchange coupling constants. Thus, the electronic absorption spectra, which represent a weighted distribution of all accessible torsional conformations in solution, correlate remarkably well with the effects of individual D-B and B-A bond torsions determined from the solid-state structures determined by X-ray crystallography.

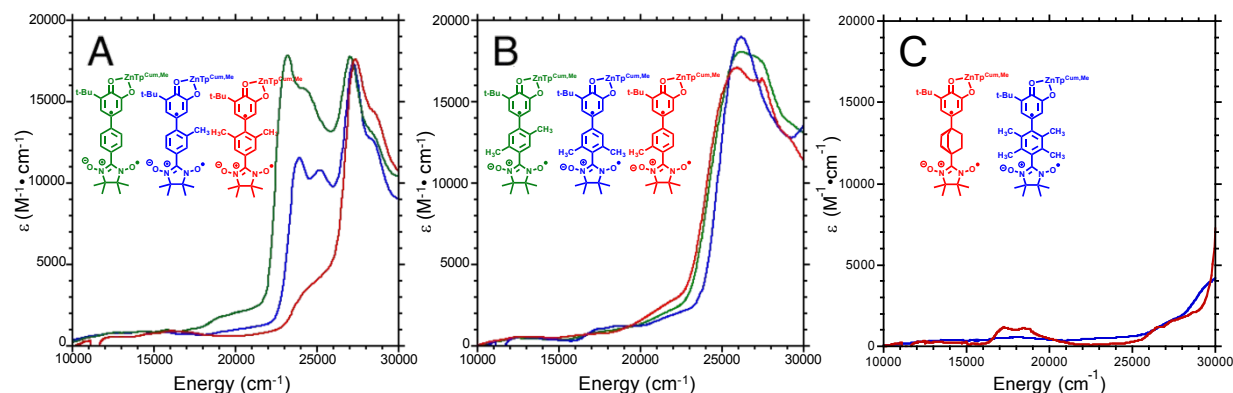


**Figure 5.** Solution electronic absorption spectra ( $\text{CH}_2\text{Cl}_2$  at 298K) for all complexes: (A) **1-Ph**, **1-MePh** and **1-Me<sub>2</sub>Ph**; (B) **1-p-MePhMe**, **1-PhMe<sub>2</sub>** and **1-PhMe**; (C) **1-BCO** and **1-Me<sub>2</sub>PhMe<sub>2</sub>**.

Our magnetic susceptibility and electronic absorption data clearly show that the conformation of the phenylene bridge relative to both the SQ and NN radical moieties is critically important in defining the magnitude of the donor-bridge-acceptor  $\pi$ -coupling and the nature of the ILCT spectral features. Resonance Raman spectroscopy is a powerful tool for probing the nature of excited state distortions relative to the equilibrium ground-state geometry, and can therefore be used to probe the role of the bridge and the degree of donor-acceptor coupling through the observation of resonantly-enhanced bridge modes.<sup>5, 32</sup> With respect to **1-Ph**, rR spectroscopy has shown that vibrations in the 1,200–1,590  $\text{cm}^{-1}$  region derive from SQ and NN in-plane stretching vibrations, and the most resonantly-enhanced Raman band is observed at  $\sim 1,600 \text{ cm}^{-1}$ . This  $\sim 1,600 \text{ cm}^{-1}$  band has been rigorously assigned as the in-plane Ph(8a)-SQ stretching vibration, where the phenylene bridge component of this stretching frequency is similar to the  $\nu_{8a}$  quinoidal stretch of the doubly degenerate benzene  $e_{2g}$  vibration.

A rR excitation profile has been constructed for the  $\sim 1,600 \text{ cm}^{-1}$  SQ-Ph(8a) quinoidal stretch of **1-MePh** (Fig. 6A) that clearly displays resonance enhancement of this mode as the laser is tuned into the ILCT band. This profile is similar to that constructed for **1-Ph** and indicates that the observed resonance enhancement derives from a dominant excited state distortion along the SQ-Ph(8a) quinoidal stretching coordinate in the ILCT excited state. The reason for resonant enhancement of this vibration becomes apparent by observing the nature of the donor (SQ SOMO) and acceptor (Ph(8a) + NN LUMO) Kohn–Sham orbitals, Fig. 6B, that are associated with the SQ( $\pi$ )SOMO  $\rightarrow$  NN-Ph( $\pi^*$ ) one electron promotion character that dominates in the ILCT excited state. In addition to **1-Ph** and **1-MePh**, the Ph(8a)-SQ quinoidal stretch is also observed in the rR spectra of **1-PhMe**, and **1-p-MePhMe** (Fig. 7) but with reduced relative intensity compared to the vibrations in the 1,200 – 1,590  $\text{cm}^{-1}$  region. The number of vibrations in the 1,200 – 1,590  $\text{cm}^{-1}$  region of the rR spectra for **1-Ph**, **1-MePh**, **1-PhMe**, and **1-p-MePhMe**, and their frequency positions are all distinctly different and reflect how the SQ and NN in-plane vibrations are affected by progressively decoupling them from the phenylene bridge as a function of the SQ-Ph and Ph-NN bond torsions. The order (**1-Ph** > **1-MePh** > **1-PhMe** > **1-p-MePhMe**) of reduced rR intensity for the SQ-Ph(8a) quinoidal stretch tracks with the decrease in exchange coupling within this series and correlates with the magnitude of SQ-Ph and Ph-NN bond torsions, reflecting the progressive resonance inhibition across the series. The results underscore the importance of a highly delocalized LUMO that can serve as the acceptor orbital in electronic excitations that originate from the SQ SOMO, since the SQ(SOMO)  $\rightarrow$  B-NN(LUMO) one-electron promotion figures prominently in the VBCI description of magnetic exchange in these donor-bridge-acceptor biradicals (Fig. 1).

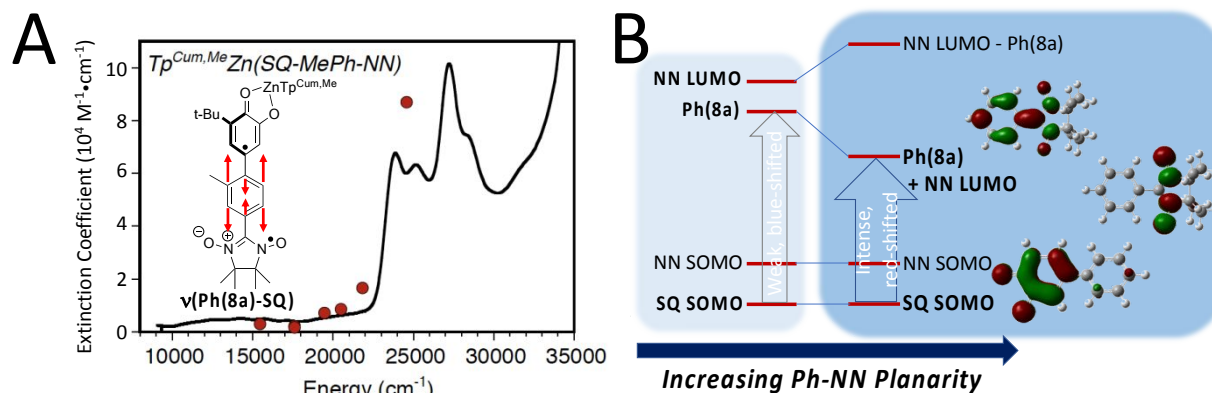


**Figure 6. A:** Resonance Raman profile (•) for **1-MePh** showing enhancement of the Ph(8a)-SQ quinoidal stretch (Me substituent not shown for clarity) in the ILCT portion of the electronic absorption spectrum (—). Raman enhancement of the quinoidal stretch is relative to the  $Na_2SO_4$  internal standard. **B:** Frontier Kohn-Sham orbital fragments that figure prominently in the ILCT transition (vertical grey arrows) and in the VBCI mechanism for magnetic exchange coupling. Dominant SQ-Ph and Ph-NN fragment orbital contributions are shown for simplicity: Note that the LUMO is predominantly the *bonding* combination of NN LUMO and bridge (phenylene) LUMO.

A plot of the relative Raman intensity for the  $\sim 1600\text{ cm}^{-1}$  SQ-Ph(8a) quinoidal stretch as a function of  $J_{SQ-B-NN}$  is presented in Fig. 7B. The “break” in the data points occurs  $\sim 75\text{ cm}^{-1}$ , and this corresponds to the methyl group substitution pattern changes between the Category A complexes ( $J_{SQ-B-NN} > 70\text{ cm}^{-1}$ ) and the Category B complexes ( $J_{SQ-B-NN} < 70\text{ cm}^{-1}$ ), effectively highlighting the sensitivity of the resonance enhancement as it relates to SQ-B vs. B-NN bond torsions.

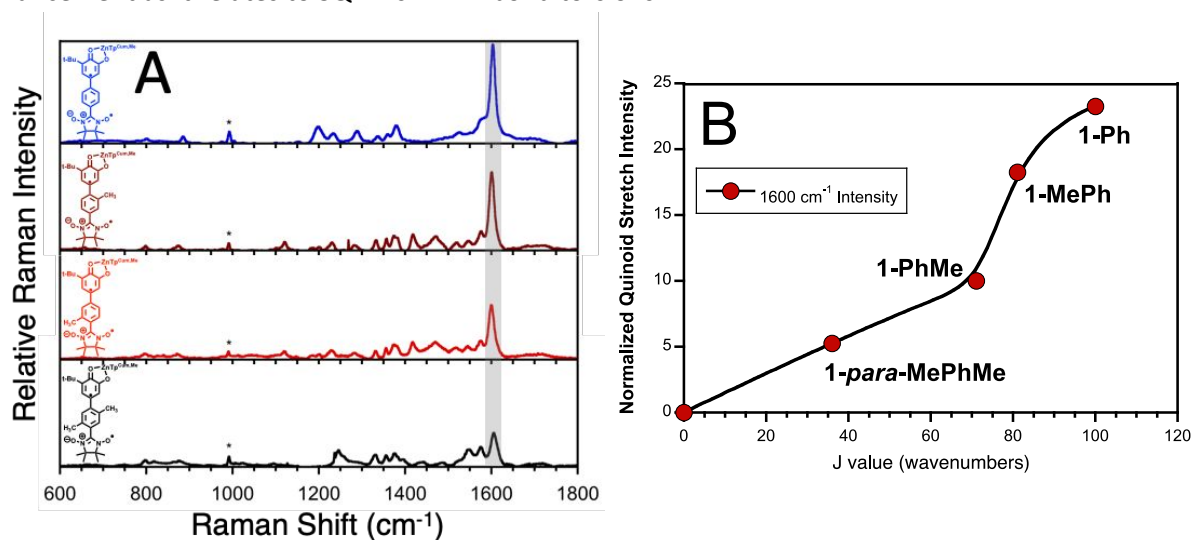


**Figure 7. A:** From top to bottom: Solid state (asterisk:  $Na_2SO_4$  internal standard) resonance Raman spectra for **1-Ph**, **1-MePh**, **1-PhMe**, and **1-p-MePhMe**;  $\lambda_{ex} = 407\text{ nm}$ . Note the reduced intensity of the  $\sim 1,600\text{ cm}^{-1}$  Ph(8a)-SQ quinoidal stretch (highlighted grey) as a function of the different **SQ-Ph** and **Ph-NN** ring-ring torsion angles indicating the effect of inhibiting extended conjugation as a function of these bond torsions. These data have been normalized to the  $800\text{ cm}^{-1}$  peak, which is tentatively assigned as an in-plane SQ stretch, for comparative

purposes. **B:** Intensity of the Ph(8a)-SQ quinoidal stretch for these compounds as a function of the magnetic exchange coupling,  $J_{\text{SQ-B-NN}}$ . The point at the origin is the quinoidal rR enhancement expected when the SQ and NN moieties are completely decoupled, and solid line is simply a guide to the eye.

## Conclusions

Donor-Bridge and Bridge-Donor bond torsions in molecular donor-bridge-acceptor triads dramatically affect both electronic and magnetic D-A couplings by modulating the relative contributions of bridge-mediated  $\sigma$ - and  $\pi$ -orbital pathways. These effects are important for increasing our understanding of bond-torsion induced inhomogeneities in experimentally determined exchange couplings, electron transfer rates, and electron transport conductance measurements. In order to explore the effects of Donor-Bridge and Bridge-Acceptor torsional rotations on electronic and magnetic coupling, we have spectroscopically and magnetically interrogated a series of Donor-phenylene-Acceptor biradical compounds that are modified only by the judicious placement of different numbers of methyl substituents on the *p*-phenylene bridge fragment. This allows for the bond torsion effects on magnetic and electronic coupling to be probed at high resolution and at parity of donor, acceptor, donor-acceptor distance, and the  $\pi$ -orbital nature of the bridge fragment.

Electronic absorption spectra of complexes with sufficient steric interactions between the donor and bridge and/or the acceptor and bridge display dramatically modified ILCT bands relative to **1-Ph**. In our SQ-*p*-phenylene-NN biradicals, torsion of the bridge-NN bond can be distinguished from torsion of the SQ-bridge bond by the energies and band-shapes of the ILCT band and the  $\sim 27000 \text{ cm}^{-1}$  B-NN( $\pi$ - $\pi^*$ ) band. Torsions about the SQ-B bond only result in a less intense and blue-shifted ILCT band, with the intense and structured B-NN( $\pi$ - $\pi^*$ ) band remaining constant. In contrast, torsions about the B-NN bond result in merged ILCT and B-NN( $\pi$ - $\pi^*$ ) bands. When the phenylene bridge is orthogonal to the SQ donor and NN acceptor (*i.e.* **1-Me<sub>2</sub>PhMe<sub>2</sub>**) these charge transfer features are dramatically attenuated. This is supported by the charge transfer spectrum of **1-BCO**, which does not possess a bridge capable of  $\pi$ -mediated electronic coupling with SQ and NN. Thus, electronic absorption spectroscopy provides a unique and powerful probe of D-B-A electronic structure as a function of differential bond torsions, allowing for one to distinguish the effects of spectral changes as a consequence of the SQ-B torsion from those of the B-NN torsion (compare Fig 3A to 3B). These individual electronic effects are not revealed by the magnitude of  $J_{\text{SQ-B-N}}$ , since this exchange parameter reflects the effects of *both* SQ *and* NN torsions relative to the bridge that combine to attenuate  $J_{\text{SQ-B-NN}}$ , (Fig. 2, Table 1).

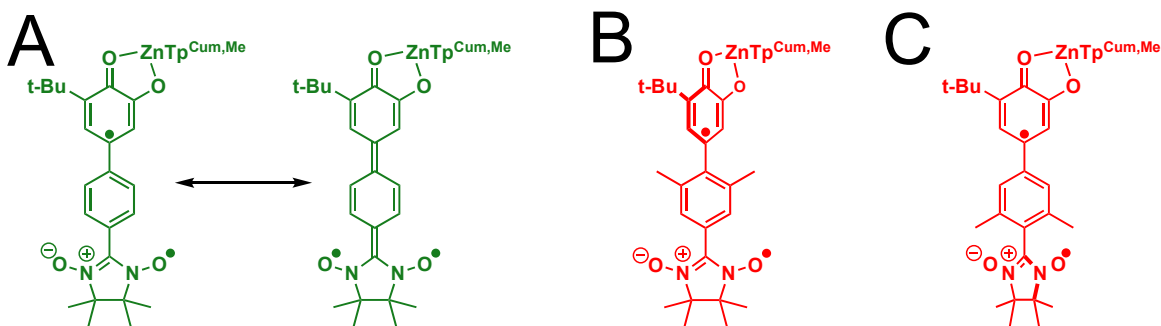


**Figure 8.** **A:** SQ-Bridge-NN conjugation maximized for no/small bond torsions between donor-bridge and between acceptor-bridge. The quinoidal resonance form (right) illustrates the vibronically-active SQ-

phenylene(8a) bridge mode. **B:** Steric inhibition of resonance for SQ donor rotated out of conjugation with bridge. **C:** Steric inhibition of resonance for NN acceptor rotated out of conjugation with bridge.

When unencumbered by steric interactions, SQ  $\rightarrow$  NN resonance delocalization as depicted in Fig. 8A describes the effects of ILCT (SQ  $\rightarrow$  B-NN) excited state character being admixed into the electronic ground state. The magnitude of this resonance delocalization effect is also revealed in the magnitude of the relative resonance enhancement for the  $\nu(\text{Ph}(8\text{a})\text{-SQ})$  quinoidal stretching mode, which is vibronically-active in the ILCT transitions (Fig. 7). Thus, the two resonance structures in Fig. 8A represent limiting valence-bond descriptions of the ground state (GS) and the ILCT excited state (EC) within the two-state VBCI formalism of Fig. 1 in the absence of any electronic coupling ( $H_{DA}$ ). Configuration interaction provides a mechanism for admixing quinoidal structure into the ground state wavefunction and enhancing the electronic coupling. The degree of quinoidal character in the ILCT excited state (EC) is conveniently probed by rR spectroscopy, which provides a convincing picture of the change in electronic coupling by monitoring the decrease in resonance enhancement of the Ph(8a)-SQ quinoidal stretch as a function of reduced SQ-B-NN planarity (Fig. 7A, B). However, when methyl groups are positioned on the bridge to force rotation of either the SQ donor (Fig. 8B), or the NN acceptor (Fig. 8C) with respect to the bridge, contributions from this key quinoidal resonance structure to the electronic ground state are attenuated and can even be eliminated (e.g. **1-Me<sub>2</sub>PhMe<sub>2</sub>**). This effectively leads to: (1) dramatic decreases in the ferromagnetic exchange interaction ( $J_{\text{SQ-B-NN}}$ ) that couples the SQ and NN radical spins in the ground state, (2) significant changes in the optical spectra, and (3) a reduction in excited state distortions along the Ph(8a)-SQ quinoidal stretch coordinate. In summary, the use of rR and electronic absorption spectroscopies, coupled with magnetic susceptibility measurements, reveal the effects of steric inhibition of resonance in torsionally-rotated Donor-Bridge-Acceptor biradicals at high resolution to provide deep insight into orbital and configuration interaction contributions to magnetic and electronic coupling.

## ASSOCIATED CONTENT

### Supporting Information

Experimental details. Synthetic-, resonance Raman, X-ray crystallographic details, computational, and magnetic susceptibility details and data are available in the Supporting Information. This material is available free of charge via the Internet at <http://pubs.acs.org>.

## AUTHOR INFORMATION

### Corresponding Author

Martin L. Kirk ([mkirk@unm.edu](mailto:mkirk@unm.edu)), David A. Shultz ([shultz@ncsu.edu](mailto:shultz@ncsu.edu)).

### Notes

The authors declare no competing financial interests.

## ACKNOWLEDGMENT

D. A. Shultz thanks the National Science Foundation (CHE-1464085 and CHE-1764181) for financial support. M. L. Kirk acknowledges the National Science Foundation (NSF CHE-1900237) for financial support.

## REFERENCES

1. Herrmann, C., Electronic Communication as a Transferable Property of Molecular Bridges? *J. Phys. Chem. A* **2019**, *123*, 10205-10223.
2. Kirk, M. L.; Shultz, D. A.; Stasiw, D. E.; Lewis, G. F.; Wang, G.; Brannen, C. L.; Sommer, R. D.; Boyle, P. D., Superexchange Contributions to Distance Dependence of Electron Transfer/Transport: Exchange- and Electronic

Coupling in Oligo(para-Phenylene)- and Oligo(2,5-Thiophene)-Bridged Donor-Bridge-Acceptor Biradical Complexes. *J. Am. Chem. Soc.* **2013**, *135*, 17144-17154.

3. Kirk, M. L.; Shultz, D. A.; Stasiw, D. E.; Habel-Rodriguez, D.; Stein, B.; Boyle, P. D., Electronic and Exchange Coupling in a Cross-Conjugated D-B-A Biradical: Mechanistic Implications for Quantum Interference Effects. *J. Am. Chem. Soc.* **2013**, *135*, 14713-14725.

4. Kirk, M. L.; Shultz, D. A., Transition Metal Complexes of Donor-Acceptor Biradicals. *Coord. Chem. Rev.* **2013**, *257*, 218-233.

5. Kirk, M. L.; Shultz, D. A.; Depperman, E. C.; Habel-Rodriguez, D.; Schmidt, R. D., Spectroscopic Studies of Bridge Contributions to Electronic Coupling in a Donor-Bridge-Acceptor Biradical System. *J. Am. Chem. Soc.* **2012**, *134*, 7812-7819.

6. Kirk, M. L.; Shultz, D. A.; Habel-Rodriguez, D.; Schmidt, R. D.; Sullivan, U., Hyperfine Interaction, Spin Polarization, and Spin Delocalization as Probes of Donor-Bridge-Acceptor Interactions in Exchange-Coupled Biradicals. *J. Phys. Chem. B* **2010**, *114*, 14712-14716.

7. Kirk, M. L.; Shultz, D. A.; Depperman, E. C.; Brannen, C. L., Donor-acceptor biradicals as ground state analogues of photoinduced charge separated states. *J. Am. Chem. Soc.* **2007**, *129*, 1937-1943.

8. Kirk, M. L.; Shultz, D. A.; Depperman, E. C., Beyond the active-electron approximation: Origin of ferromagnetic exchange in donor-acceptor heterospin biradicals. *Polyhedron* **2005**, *24*, 2880-2884.

9. Davis, W. B.; Ratner, M. A.; Wasielewski, M. R., Conformational Gating of Long Distance Electron Transfer through Wire-like Bridges in Donor-Bridge-Acceptor Molecules. *J. Am. Chem. Soc.* **2001**, *123*, 7877-7886.

10. Vonlanthen, D.; Mishchenko, A.; Elbing, M.; Neuburger, M.; Wandlowski, T.; Mayor, M., Chemically Controlled Conductivity: Torsion-Angle Dependence in a Single-Molecule Biphenyldithiol Junction. *Angew. Chem. Int. Ed.* **2009**, *48*, 8886-8890.

11. Benniston, A. C.; Harriman, A.; Li, P.; Patel, P. V.; Sams, C. A., The effect of torsion angle on the rate of intramolecular triplet energy transfer. *Phys. Chem. Chem. Phys.* **2005**, *7*, 3677-3679.

12. Hanss, D.; Wenger, O. S., Conformational Effects on Long-Range Electron Transfer: Comparison of Oligo-p-phenylene and Oligo-p-xylene Bridges. *Eur. J. Inorg. Chem.* **2009**, (25), 3778-3790.

13. McConnell, H. M., Intramolecular charge transfer in aromatic free radicals. *J. Chem. Phys.* **1961**, *35*, 508-515.

14. Newton, M. D., Modeling Donor/Acceptor Interactions: Combined Roles of Theory and Computation. *J. Quantum Chem.* **2000**, *77*, 255-263.

15. Stasiw, D. E.; Zhang, J.; Wang, G.; Dangi, R.; Stein, B. W.; Shultz, D. A.; Kirk, M. L.; Wojtas, L.; Sommer, R. D., Determining the Conformational Landscape of  $\sigma$  and  $\pi$  Coupling Using para-Phenylene and "Aviram-Ratner" Bridges. *J. Am. Chem. Soc.* **2015**, *137*, 9222-9225.

16. Solomon, G. C.; Andrews, D. Q.; Van Duyne, R. R.; Ratner, M. A., Electron Transport through Conjugated Molecules: When the pi System Only Tells Part of the Story. *Chemphyschem* **2009**, *10* (1), 257-264.

17. Solomon, G. C.; Bergfield, J. P.; Stafford, C. A.; Ratner, M. A., When "small" terms matter: Coupled interference features in the transport properties of cross-conjugated molecules. *Beilstein J. Nanotech.* **2011**, *2*, 862-871.

18. Remington, W. R., The Effects of Steric Inhibition of Resonance on Ultraviolet Absorption Spectra. *J. Am. Chem. Soc.* **1945**, *67* (10), 1838-1842.

19. Arnold, R. T.; Peirce, G.; Barnes, R. A., The steric inhibition of resonance. *J. Am. Chem. Soc.* **1940**, *62*, 1627-1628.

20. Shultz, D. A.; Vostrikova, K. E.; Bodnar, S. H.; Koo, H.-J.; Whangbo, M.-H.; Kirk, M. L.; Depperman, E. C.; Kampf, J. W., Trends in Metal-Biradical Exchange Interaction for First-Row MII(Nitronyl Nitroxide-Semiquinone) Complexes. *J. Am. Chem. Soc.* **2003**, *125*, 1607-1617.

21. Ruf, M.; Noll, B. C.; Groner, M. D.; Yee, G. T.; Pierpont, C. G., Pocket Semiquinonate Complexes of Cobalt(II), Copper(II), and Zinc(II) Prepared with the Hydrdotris(cumenylmethylpyrazolyl)borate Ligand. *Inorg. Chem.* **1997**, *36*, 4860-4865.

22. Ruf, M.; Vahrenkamp, H., Small Molecule Chemistry of the Pyrazolylborate—Zinc Unit  $\text{Tp}^{\text{Cum,Me}}\text{Zn}$ . *Inorg. Chem.* **1996**, *35*, 6571-6578.

23. Blondin, G.; Girerd, J. J., Interplay of Electron Exchange and Electron-Transfer in Metal Polynuclear Complexes in Proteins or Chemical-Models. *Chem. Rev.* **1990**, *90* (8), 1359-1376.

24. Bertrand, P., Electron-Transfer Between Biological Molecules Coupled by an Exchange Interaction. *Chem. Phys. Lett.* **1985**, *113* (1), 104-107.
25. Herrmann, C.; Elmisz, J., Electronic communication through molecular bridges. *Chemical Communications* **2013**, 49 (89), 10456-10458.
26. Brunold, T. C.; Gamelin, D. R.; Solomon, E. I., Excited-state exchange coupling in bent Mn(III)-O-Mn(III) complexes: Dominance of the pi/sigma superexchange pathway and its possible contributions to the reactivities of binuclear metalloproteins. *J. Am. Chem. Soc.* **2000**, *122* (35), 8511-8523.
27. Wenger, O. S.; Hankache, J., Organic Mixed Valence. *Chem. Rev.* **2011**, *111*, 5138-5178.
28. Lukas, A. S.; Bushard, P. J.; Weiss, E. A.; Wasielewski, M. R., Mapping the Influence of Molecular Structure on Rates of Electron Transfer Using Direct Measurements of the Electron Spin-Spin Exchange Interaction. *J. Am. Chem. Soc.* **2003**, *125*, 3921-3930.
29. Pauling, L., *The nature of the chemical bond and the structure of molecules and crystals : an introduction to modern structural chemistry*. 3rd ed.; Cornell University Press: Ithaca, N.Y., 1960; p 644.
30. Putz, A. M.; Schatzschneider, U.; Rentschler, E., Integrated experimental and computational spectroscopy study on the protonation of the alpha-nitronyl nitroxide radical unit. *Phys. Chem. Chem. Phys.* **2012**, *14* (5), 1649-1653.
31. Osiecki, J. H.; Ullman, E. F., Studies of free radicals. I. .alpha.-Nitronyl nitroxides, a new class of stable radicals. *J. Am. Chem. Soc.* **1968**, *90*, 1078-1079.
32. Londergan, C. H.; Rocha, R. C.; Brown, M. G.; Shreve, A. P.; Kubiak, C. P., Intervalence involvement of bridging ligand vibrations in hexaruthenium mixed-valence clusters probed by resonance Raman spectroscopy *J. Am. Chem. Soc.* **2003**, *125*, 13912 -13913.



TOC GRAPHIC

